THE EFFECT OF BANDPASS UNCERTAINTIES ON COMPONENT SEPARATION

Sarah Church[1], Lloyd Knox[2] and Martin White[3]
[1]Department of Physics, Stanford University
[2]Department of Physics, University of California, Davis, CA 95616
[3]Departments of Astronomy and Physics, University of California, Berkeley, CA 94720

Draft version October 14, 2002

ABSTRACT

Multi-frequency measurements of the microwave sky can be decomposed into maps of distinct physical components such as the cosmic microwave background (CMB) and the Sunyaev–Zel'dovich (SZ) effect. Each of the multi–frequency measurements is a convolution of the spectrum on the sky with the bandpass of the instrument. Here we analytically calculate the contamination of the component maps that can result from errors in our knowledge of the bandpass shape. We find, for example, that for *Planck* an unknown 10% ramp across each band results in a CMB map $\delta T = \delta T_{CMB} - 4.3 \times 10^{-3} \delta T_{SZ}$ plus the usual statistical noise. The variance of this contaminant is more than a factor of 100 below the noise variance at all angular scales and even further below the CMB signal variance. This contamination might lead to an error in the velocity of rich clusters inferred from the kinetic SZ effect, however the error is negligible, $\mathcal{O}(50\mathrm{km\,s^{-1}})$, if the bandpass is known to 10%. Bandpass errors might be important for future missions measuring the CMB-SZ correlation.

Subject headings: cosmic microwave background – cosmology: theory – galaxies: clusters: general – large-scale structure of universe

1. INTRODUCTION

Small scale anisotropies in the cosmic microwave background can arise from a number of sources. In addition to the 'primary' anisotropies, generated at the surface of last scattering, secondary anisotropies and foregrounds can contribute to the observed brightness fluctuations. Separating the components from multi-frequency observations is an important part of the data reduction and interpretation. Here we consider the effect of uncertainties in the frequency response of the instrument within the observational bands and how that impacts our ability to perform component separation.

2. MODEL OF THE SKY

We assume for simplicity that the intensity in any given direction of the sky is the sum of 5 components. The first is the CMB itself with specific intensity

$$I_\nu = \frac{dB_\nu}{d\nu} \propto \frac{x^4 e^x}{(e^x - 1)^2} \tag{1}$$

where B_ν is a blackbody spectrum and $x = h\nu/k_B T_{CMB} \simeq \nu/56.84\mathrm{GHz}$ is the dimensionless frequency. The kinetic Sunyaev-Zel'dovich effect (SZ; Sunyaev & Zel'dovich 1972, 1980; for recent reviews see Birkinshaw 1999 and Rephaeli 1995), arising from the motion of ionized gas with respect to the rest-frame of the CMB, has the same frequency dependence as the CMB signal. The second component is the thermal SZ effect – one of the primary sources of secondary anisotropies in the CMB on small angular scales. Ignoring relativistic corrections, the change in the (thermodynamic) temperature of the CMB resulting from scattering off non-relativistic electrons is

$$\frac{\Delta T}{T} = y\left(x\frac{\mathrm{e}^x + 1}{\mathrm{e}^x - 1} - 4\right) \tag{2}$$

$$\simeq -2y \qquad \text{for} \quad x \ll 1\,, \tag{3}$$

where the second expression is valid in the Rayleigh-Jeans limit and y is the Comptonization parameter which is proportional to the integrated electron pressure along the line of sight.

We also include dust, bremsstrahlung (or free-free) emission and synchrotron radiation following Knox (1999, see below). Specifically for the dust we assume the spectral dependence of a modified blackbody with an emissivity index of 2 and a temperature of 18K. For the bremsstrahlung and synchrotron we assume power-laws in frequency with indices −0.16 and −0.8 respectively (Bennett et al. 1992). Our model does not include a contribution from extragalactic point sources. For the purposes of this analysis we hold the spectral indices of the components fixed (and known). Though we do not expect this to be true of real

Number	Frequency	$\Delta\nu/\nu$	Beam	Noise
1	30	0.2	33	5.5
2	44	0.2	24	7.4
3	70	0.2	14	13
4	100	0.2	10	21
5	100	0.3	9.2	5.5
6	143	0.3	7.1	6
7	217	0.3	5.0	13
8	353	0.3	5.0	40
9	545	0.3	5.0	400

Table 1
The parameters assumed for *Planck*. The central frequency is quoted in GHz, the beam size in arcminutes and the noise (thermodynamic temperature fluctuation in a square pixel of side 'Beam') in μK assuming a 12 month integration. We do not use the 850GHz channel of *Planck* here since our focus is on components at lower frequency.

astrophysical foregrounds, the impact of this on our analysis is negligible.

3. METHOD

To understand the effect of an uncertainty in the response of the instrument to a particular signal let us postulate the following situation. We imagine that the sky is observed at N frequencies, with measurements θ_i ($i = 1, \cdots, N$). The signal is the sum of M components with amplitudes s_α ($\alpha = 1, \cdots, M$) such that

$$\theta_i = \sum_\alpha f_{i\alpha} s_\alpha + n_i \tag{4}$$

where n_i is the noise in channel i. We write our linear estimator of s_α as

$$\widehat{s}_\alpha = \sum_i W_{i\alpha} \theta_i \quad . \tag{5}$$

Requiring $\widehat{s}$ to be an unbiased estimator and minimizing the rms residual, $\langle(\widehat{s} - s)^2\rangle$, gives

$$W_{i\alpha} = \sum_{\beta j} F^{-1}_{\alpha\beta} f_{j\beta} N^{-1}_{ji} \tag{6}$$

where $N_{ij} \equiv \langle n_i n_j \rangle$ and $F_{\alpha\beta} = \sum_{ij} f_{i\alpha} N^{-1}_{ij} f_{j\beta}$ is the Fisher matrix for the s_α. In the case of diagonal noise, $N_{ij} = \sigma_i^2 \delta_{ij}$, the Fisher matrix simplifies to

$$F_{\alpha\beta} = \sum_i f_{i\alpha} f_{i\beta} / \sigma_i^2 \tag{7}$$

and the estimator can be written as

$$\widehat{s}_\alpha = \sum_{i\beta} F^{-1}_{\alpha\beta} \frac{f_{i\beta}}{\sigma_i^2} \theta_i. \tag{8}$$

The covariance matrix of the statistical errors for this estimator is $\langle(\hat{s}_\alpha - s_\alpha)(\hat{s}_\beta - s_\beta)\rangle = F^{-1}_{\alpha\beta}$.

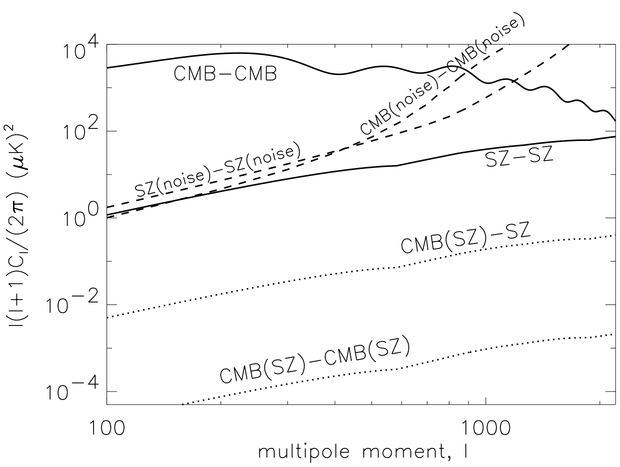

FIG. 1.— The angular power spectra, $\ell(\ell+1)C_\ell/(2\pi)$, of the CMB and thermal SZ signals (solid) fluctuations and the CMB and thermal SZ map noise (dotted). The tSZ contamination of the CMB map, CMB(SZ), correlated with itself (with SZ) are shown as the dotted curves. We assumed a 10% ramp error on all *Planck* bandpasses.

We are interested in the effects on our component separation of a band error which causes the actual bandpass to deviate from the design bandpass by δf. Using Eq. (8) with the design bandpass, but replacing θ_i with the right-hand side of Eq. (4) evaluated with the actual bandpass, and subtracting off the true signal we find

$$\delta s_\alpha \equiv \langle \widehat{s}_\alpha - s_\alpha \rangle = \sum_\beta M_{\alpha\beta} s_\beta \tag{9}$$

where M is the 'component mixing matrix' given by

$$M_{\alpha\beta} \equiv \sum_{i\gamma} F^{-1}_{\alpha\gamma} \frac{f_{i\gamma} \delta f_{i\beta}}{\sigma_i^2} \tag{10}$$

and $\delta f_{i\beta}$ is the difference between the design and actual bandpasses. The bandpass uncertainty then induces a relative rms error on component α from component β characterized by

$$W_{\alpha\beta} \equiv \frac{M_{\alpha\beta} \langle s_\beta^2 \rangle^{1/2}}{\langle s_\alpha^2 \rangle^{1/2}} \quad . \tag{11}$$

How is $\delta f_{i\alpha}$ related to the bandpass error? If component α has frequency dependence $g_\alpha(\nu)$ then

$$f_{i\alpha} = \int d\nu \; g_\alpha(\nu) \Big[h_i(\nu) + \delta h_i(\nu) \Big] \tag{12}$$

where $h_i(\nu) + \delta h_i(\nu)$ is the total bandpass, with the latter term the error. It is easy to see that an error in the amplitude of the bandpass, $\delta h_i(\nu) \propto h_i(\nu)$, will have no effect on component separation since it will 'calibrate out'. In general we shall model this calibration process by demanding that

$$f_{i0} = \int d\nu \; g_0(\nu) \Big[h_i(\nu) + \delta h_i(\nu) \Big] = 1 \quad \forall i \tag{13}$$

where component 0 is the CMB. We normalize $g_\alpha(\nu = 30 \text{ GHz}) = 1$ for all components α. Note that this means s_α is the amplitude of component α at 30 GHz.

Note that the above treatment applies in both pixel space and spherical harmonic space. In pixel space the σ_i should all be calculated for the same pixel size. In spherical harmonic space, the σ_i (interpreted as errors on the beam–deconvolved maps) are ℓ–dependent:

$$\sigma_i(\ell) = \hat{\sigma}_i \vartheta_i \exp\left[\frac{1}{2} \left(\frac{\ell \vartheta_i}{2.355} \right)^2 \right] \tag{14}$$

where ϑ and $\hat{\sigma}$ are the beam and noise defined in Table 1 with ϑ converted to radians.

4. RESULTS

As an example let us consider simple shifts in the bandpass, which we shall model as a top-hat of width $\Delta\nu$ about the central frequency as given in Table 1. To gain intuition let us restrict ourselves to a 2×2 subspace consisting only of CMB and tSZ signals with a 1GHz shift in the 217GHz channel to higher frequency. In this case (at angular scales larger than the largest beam)

$$M_{\alpha\beta} = \begin{pmatrix} 0.0 & -0.00391 \\ 0.0 & 0.00522 \end{pmatrix} \tag{15}$$

	CMB	tSZ	Dust	Sync	Brem
CMB	0.0	-4.3×10^{-3}	-2.5×10^{-1}	8.3×10^{-5}	1.4×10^{-5}
tSZ	0.0	3.7×10^{-3}	6.4×10^{-1}	-2.2×10^{-4}	-8.6×10^{-5}
Dust	0.0	7.2×10^{-7}	2.1×10^{-2}	8.6×10^{-7}	4.7×10^{-8}
Sync	0.0	6.9×10^{-3}	-4.3	-2.6×10^{-3}	4.1×10^{-4}
Brem	0.0	-6.3×10^{-3}	4.0	-8.1×10^{-4}	-4.9×10^{-3}

Table 2

The component-mixing matrix, $M_{\alpha\beta}$, for a 5 component model (cmb, sz, dust, synchroton, bremsstrahlung) if all of the frequency channels have an undetected +10% ramp (see text).

	CMB	tSZ	Dust	Sync	Brem
CMB	0.0	-0.00032	-0.00005	0.00001	0.00000
tSZ	0.0	0.00355	0.00644	-0.00019	-0.00019
Dust	0.0	0.00002	0.02191	0.00010	0.00010
Sync	0.0	0.01387	-0.09358	-0.00373	0.00373
Brem	0.0	-0.00747	0.05165	-0.00025	-0.00025

Table 3

The normalized mixing matrix, $W_{\alpha\beta}$, for a 5 component model (cmb, sz, dust, synchroton, bremsstrahlung) if all of the frequency channels have an undetected +10% ramp (see text).

which indicates that the CMB channel does not 'contaminate' the any of the signals but there is leakage from the tSZ channel. That $M_{\alpha 0} = 0$ is a direct result of our calibration procedure which enforces $\delta f_{i0} = 0$. Note that for other calibration sources typically used by ground–based experiments, e.g. planets, the CMB *can*, via bandpass errors, contaminate other components.

A more realistic scenario is that the bandpass frequency be quite well determined, but the amplitude of the response as a function of frequency be somewhat uncertain. This holds for both HEMTs (M. Seiffert, private communication) and Bolometers (P. Ade, private communication). As a simple model of this effect we introduce a linear 'ramp' into our otherwise top-hat bandpasses with a change in amplitude of 10% across the band. The results of including a +10% ramp in all of the channels with our 5 component model is given in Table 2.

The elements of the mixing matrix in Table 2 tell us, for example, that our CMB map, $\hat{s}_0$ will have a contribution from dust of $-0.25 s_2$, where s_2 is the dust amplitude at 30 GHz. Fortunately the dust amplitude is very low at 30 GHz!

The importance of this contamination is easier to read from the normalized mixing matrix, $W_{\alpha\beta}$. To calculate $W_{\alpha\beta}$ we need to know the rms sky fluctuations of the various components. We use the model described in Knox (1999) and references therein, most notably Bouchet & Gispert (1999). The exception is our SZ power spectrum which we take from White, Hernquist & Springel (2002) and extend to $\ell < 400$ by assuming $C_\ell = C_{400}$ appropriate for the Poisson dominated regime (see Fig. 1).

In Table 3 we assume s_α are the amplitudes of an $\ell = 500$ spherical harmonic, so that $\langle s_\alpha^2 \rangle = C_\ell^\alpha$. We find that all the elements are quite small; the largest contribution to the CMB map comes from SZ and the rms of this contaminant is .05% of the CMB signal rms. The galactic contaminants of the CMB map, $W_{0\beta}$ for $\beta = 2, 3, 4$ greatly increase with increasing angular scale. Even so, they are very small at all angular scales; at $\ell = 2$ $W_{0\beta}$ = -0.006, 0.0002 and 2×10^{-5} for dust, synchrotron and bremstrahlung respectively.

In Fig. 1 we show how the SZ contamination of the CMB map affects the CMB power spectrum and the CMB-SZ cross–correlation power spectrum. Denoting the CMB contaminant from SZ as $a_{lm}^{\rm CMB(SZ)}$ we have

$$C_\ell^{\rm CMB(SZ)-SZ} \equiv \langle a_{\ell m}^{\rm CMB(SZ)} (a_{\ell m}^{\rm SZ})^* \rangle = M_{01}(\ell) C_\ell^{\rm SZ-SZ}. \tag{16}$$

The ℓ-dependence of the mixing matrix arises from the ℓ-dependence of the noise in the beam–deconvolved maps but is quite mild: $M(0,1)$ monotonically decreases from -4×10^{-3} to its high ℓ asymptote of -5.3×10^{-3}. In general the cross–correlations are the most affected since they are first order in the component mixing matrix. Fortunately, for the 10% ramp error, the bandpass error–induced cross–correlation is well below the level of the *Planck* noise.

Our results are specific to the conservative component separation procedure we have assumed. Other methods can reduce the statistical noise by including assumptions about the statistical properties of the various components (Tegmark & Efstathiou 1996; Bouchet, Gispert & Puget 1995; Hobson et al. 1998). The results will also differ in detail if one adopts a more realistic (and more complicated) model of the foregrounds. However, we do not expect the component mixing matrix to be qualitatively different for these different procedures or for more realistic foreground modeling. The fact that the two–component model and the five–component model give similar results for both $M(0,1)$ and $M(1,1)$ we take as evidence of this robustness.

The bandpass uncertainties can lead to systematic errors in the velocities of clusters inferred from the kinetic SZ effect. The mixing between thermal SZ and primary CMB on a cluster of optical depth τ and temperature T_e induces an error

$$\delta T \simeq -8 \times 10^{-3}\ \tau \left(\frac{kT_e}{m_e c^2}\right) \tag{17}$$

in the CMB signal. If the contamination were all erroneously attributed to kinetic SZ from the moving cluster, it would bias the inferred velocity by $v = 8 \times 10^{-3}(kT_e/m_ec^2)c \approx 50\mathrm{km\,s}^{-1}$ for a rich cluster. This bias is negligible compared to other sources of uncertainty for individual cluster velocities (Haehnelt & Tegmark 1996, Nagai et al. 2002, Holder 2002) but is comparable to errors that might be achievable by *Planck* on bulk flows in 10^6h^{-3} Mpc^3 volumes (Aghanim et al. 2001). This systematic contaminant of the bulk flows will appear as a T_e–weighted monopole. Such a pattern is not expected cosmologically, would be evidence of bandpass errors and could be removed from the data with negligible residuals. Note that while we have ignored relativistic corrections to the SZ distortion for the purposes of estimating the magnitude of the effect, they will be important in the actual analysis of the data (Diego et al. 2002).

5. CONCLUSIONS

We can conclude that bandpass errors at the $\mathcal{O}(10\%)$ level are acceptably small for *Planck*. More sensitive experiments though may have more stringent requirements on the quality of the bandpass measurements because an overall scaling of the sensitivity of each channel leaves the component mixing matrix unchanged.

We thank P. Ade, G. Holder, C. Lawrence and M. Seiffert for useful conversations. M.W. was supported by a NASA Astrophysical Theory Grant, the NSF and a Sloan Fellowship. L.K. was supported by NASA NAG5-11098. We thank the KITP (supported by NSF PHY99-07949) for their hospitality.

REFERENCES

Aghanim, N., Gorski, K., Puget, J.-L., 2001, å, 374, 1
Bennett C.L., et al., 1992, ApJ, 396, L7
Birkinshaw M., 1999, Phys. Rep., 310, 98
Bouchet, F.R., Gispert, R., Puget, J.-L., 1995, The mm/sub-mm Foregrounds and Future CMB Space Missions, in "Unveliing the Cosmic Infrared BAckground", AIP Conference Proceedings 348, ed. E. Dwek (Baltimore, MD, USA: pages 255-268)
Bouchet, F., Gispert, R., 1999, New Astronomy, 4, 443
Diego, J.M., Hansen, S.H., Silk, J., astro-ph/0207178
Haehnelt, M., Tegmark, M., 1996, MNRAS279 545
Hobson, M.P., Jones, A.W., Lasenby, A.N., Bouchet, F.R., 1998, MNRAS 300, 1
Holder, G., astro-ph/0207600
Knox L., 1999, MNRAS., 307, 977
Nagai, D. Kravtsov, A.V., Kosowsky, A., astro-ph/0208308
Ostriker J.P., Vishniac E.T., 1986, ApJ, 306, L51
Rephaeli Y., 1995, ARA&A, 33, 541
Sunyaev R.A., Zel'dovich Ya. B., 1972, Comm. Astrophys. Space Phys., 4, 173
Sunyaev R.A., Zel'dovich Ya. B., 1980, ARA&A, 18, 537
Tegmark, M., Efstathiou, G., 1996, MNRAS, 281, 1297
White M., Hernquist L., Springel V., 2002, ApJ, in press [astro-ph/0205437]